Available online at www.sciencedirect.com
SCIENCE DIRECT
Journal of Photochemistry and Photobiology A: Chemistry 180 (2006) 15–22
Journal of Photochemistry and Photobiology A:Chemistry
www.elsevier.com/locate/jphotochem

Photocatalytic degradation of formic and benzoic acids and hydrogen peroxide evolution in TiO_2 and ZnO water suspensions

Marta Mrowetz, Elena Selli *

Dipartimento di Chimica Fisica ed Elettrochimica, Università degli Studi di Milano, Via Golgi 19, I-20133 Milano, Italy

Received 19 April 2005; received in revised form 5 September 2005; accepted 8 September 2005
Available online 13 October 2005

Abstract

The photocatalytic degradation of formic acid (FA) and benzoic acid (BA), chosen as model organic molecules with acidic properties, was investigated in TiO_2 and ZnO water suspensions under different experimental conditions. Hydrogen peroxide evolution, formed through a reductive pathway started by conduction band electrons, was also simultaneously monitored during the degradation runs. The effect of different initial amounts of substrates and the dependence of the reaction rate on the initial pH of the TiO_2 suspensions was interpreted under the light of a pseudo-steady state Langmuir–Hinshelwood rate form and of the electrostatic interactions occurring at the water–semiconductor interface. ZnO appeared a more effective photocatalyst than TiO_2 for BA, but not for FA degradation. A much higher amount of hydrogen peroxide was detected in ZnO irradiated suspensions, both in the presence and in the absence of the substrates, mainly because of its lower photocatalytic decomposition rate on such oxide. The rate of hydrogen peroxide evolution during the photocatalytic oxidation of BA on TiO_2 could be related to the rate of the oxidation process, while H_2O_2 could not be detected during the photocatalytic degradation of FA on this oxide, mainly because of the reduced shielding ability of this substrate.

Keywords: Photocatalytic degradation; Formic acid; Benzoic acid; Titanium dioxide; Zinc oxide; Hydrogen peroxide

1. Introduction

In recent years, many studies have been focused on the photocatalytic degradation of organic compounds mediated by semiconductor particles acting as photocatalysts [1–3]. In particular, titanium dioxide has been widely employed, thanks to its outstanding photocatalytic activity and high stability. Among other widely investigated semiconductors, zinc oxide also shows a high efficiency in photocatalysis, even if its low stability, which makes its aqueous suspensions stable only at basic pH, represents a strong limitation to its practical use [4,5]. The efficiency of photocatalytic processes has been shown to depend on several different characteristics of the semiconductor particles, such as their surface properties, the position of their band gap potentials, the mobility and recombination rate of the charge carriers generated by UV-light absorption. Moreover, a relevant role is also played by the chemical and adsorption properties of the degradation substrate, depending also on experimental conditions, such as pH and the substrate to photocatalyst concentration ratio.

The photocatalytic degradation of organic pollutants having direct relevance in water remediation treatments, i.e. 2-chlorophenol, a couple of acid azo dyes and the gasoline additive methyl *tert*-butyl ether, has been recently investigated by us [6–9]. In the present work, the interest was focused on the photocatalytic degradation of formic acid (FA) and benzoic acid (BA), two model compounds suitable for investigating the photocatalytic behaviour of aliphatic and aromatic organic acids, respectively. In particular, FA was chosen because it undergoes direct mineralisation to CO_2 and H_2O without the formation of any stable intermediate species [10–13]. Moreover, it also represents a possible final step in the photodegradation of more complex organic compounds. BA is a particularly suitable model molecule for understanding the photocatalytic behaviour of more complex aromatic water pollutants with acidic properties, initially undergoing hydroxylation of the benzene ring under photocatalytic conditions [14–16].

* Corresponding author. Tel.: +39 02 503 14237; fax: +39 02 503 14300.
E-mail addresses: marta.mrowetz@unimi.it (M. Mrowetz), elena.selli@unimi.it (E. Selli).

1010-6030/$ – see front matter © 2005 Elsevier B.V. All rights reserved.
doi:10.1016/j.jphotochem.2005.09.009

The photocatalytic degradation of the two substrates was investigated in the presence of titanium dioxide and of zinc oxide under different experimental conditions. In particular, the effects of pH and of the initial substrate concentration were investigated in relation to the adsorption properties of the two substrates on the semiconductors. The evolution of hydrogen peroxide, formed by reduction of adsorbed molecular oxygen by conduction band electrons, was also monitored during the photodegradation runs; this gave information on the rate of the main reduction path occurring in parallel to the photocatalytic oxidative degradation of the two organic acids.

2. Experimental

2.1. Materials

Formic acid (purity 95–97%) and benzoic acid (purity >99.5%) were purchased from Aldrich. Titanium dioxide (Degussa P25, measured surface area 35 $m^2\,g^{-1}$ [17]) and zinc oxide (Fluka, surface area 5 $m^2\,g^{-1}$) were employed as photocatalysts. All other chemicals were high purity Aldrich products. Water purified by Milli-Q water system (Millipore) was used throughout.

2.2. Apparatus

All degradation runs were carried out at $35 \pm 1\,^{\circ}C$ in a 400 mL cylindrical Pyrex closed reactor under magnetic stirring, by employing an experimental set-up similar to that already described [8,17]. Irradiation was performed by means of a 250 W iron alogenide lamp (Jelosil, model HG 200) emitting in the 315–400 nm wavelength range; its emission intensity on the reactor was 3.4×10^{-7} Einstein $s^{-1}\,cm^{-2}$, as periodically checked by ferrioxalate actinometry [18].

2.3. Procedure

Aqueous suspensions employed in photocatalytic runs usually contained 0.1 g L^{-1} of TiO_2 or ZnO and a 5.0×10^{-4} M initial concentration of FA or a 1.0×10^{-4} M initial concentration of BA. The lamp was always switched on at least 30 min before the beginning of irradiation. All kinetic runs were performed under atmospheric conditions and constant magnetic stirring, as previously described [7,8]. Under so called natural pH conditions neither acids nor bases were added to TiO_2 suspensions, to avoid any possible interference of other species (mainly anions) on the photoredox reactions at the semiconductor–water interface. During the degradation runs under such conditions the pH increased, from an initial value of 3.5 to a final value of ca. 5.8 for FA and from 4.2 to ca. 6.0 for BA. On the contrary, when investigating the effects of different pH conditions, $HClO_4$ and NaOH or a 10^{-2} M NH_3/NH_4NO_3 buffer solution were added to adjust the pH of the suspensions. Both ClO_4^- and NO_3^- anions are expected to have negligible influence on the photocatalytic processes, because of their poor adsorption on the semiconductor surface and their low affinity for $^{\bullet}OH$ radicals [19]. When ZnO was employed as photocatalyst, the pH of the suspension was always maintained above 8.5, thus ensuring the photostability of the semiconductor oxide [20].

FA photodegradation was monitored by means of total organic carbon (TOC) analysis in the not purgeable organic carbon (NPOC) mode, employing a TOC-5000A Shimadzu instrument. BA concentration during the runs was detected by HPLC analysis, employing an Agilent 1100 Series apparatus, equipped with a μBondapak-C18 column and a UV–vis detector ($\lambda = 230$ nm). A water:methanol 72:28 mobile phase was used, flowing at 0.8 mL min^{-1}. Absorption spectra were successively recorded during BA photodegradation ($\lambda_{max} = 225$ nm) by means of a Perkin-Elmer Lambda 16 apparatus [8] and the extent of mineralisation was also determined by TOC analysis. The photocatalyst particles were removed by centrifugation at 3000 rpm for 30 min prior to any analytical determination on the samples (2 mL) periodically withdrawn from the irradiated suspensions. All runs were repeated at least twice to check their reproducibility.

The hydrogen peroxide concentration was monitored during the photodegradation runs by a fluorimetric analysis ($\lambda_{ex} = 316.5$ nm, $\lambda_{em} = 408.5$ nm) of the fluorescent dimer formed in the horseradish peroxidase catalysed reaction of H_2O_2 with *p*-hydroxyphenylacetic acid [21,22], using a 650-10S Perkin-Elmer fluorescence spectrophotometer. Hydrogen peroxide standard solutions employed in calibration were analysed iodometrically.

Adsorption tests of the two acids were performed in aqueous suspensions containing 1.0 g L^{-1} of TiO_2 at different pH or 1.0 g L^{-1} of ZnO at basic pH, which had been maintained in the dark under constant stirring at 35 °C for 24 h. The fraction of FA and BA adsorbed on the photocatalyst was determined by TOC and spectrophotometric analysis, respectively, after removal of the powder by filtration through Millipore 0.22 μm disks and by centrifugation.

3. Results and discussion

3.1. Adsorption equilibria involving FA and BA

Preliminary studies of FA and BA adsorption on titanium dioxide and zinc oxide were performed in suspensions containing a standard initial concentration of the two acids and an amount of the two oxides which was 10-fold higher than that employed in the photocatalytic runs. The extent of FA adsorption on the surface of both oxides was always found to be negligible, in agreement with previous data [23,24]. Very recent FA adsorption measurements, performed in the presence of a higher amount of TiO_2 P25 than that of the present study [24], predict in fact a less than 0.05 ppm concentration decrease in the aqueous phase due to FA adsorption under our conditions, which of course would be undetectable.

On the contrary, BA adsorption was not negligible on 1.0 g L^{-1} of titanium dioxide. As shown in Table 1, maximum adsorption occurred under natural pH conditions, while the BA adsorbed fraction was lower at lower pH and no adsorption could be detected on both TiO_2 and ZnO at basic pH. The observed trend clearly reflects the electrostatic interactions at the

Table 1
Fraction of benzoic acid ($C^0_{BA} = 1.0 \times 10^{-4}$ M) adsorbed on titanium dioxide (1.0 g L^{-1}) and zinc oxide (1.0 g L^{-1}) under different pH conditions

Photocatalyst	pH	Adsorbed fraction
TiO_2	2.6	0.08
TiO_2	3.6	0.09
TiO_2	4.2	0.31
TiO_2	9.0	<0.001
ZnO	9.0	<0.001

semiconductor–water interface, depending on the surface charge of TiO_2 and, at the same time, on the extent of BA deprotonation ($K_a = 6.46 \times 10^{-5}$ at 298 K). In fact, at natural pH (ca. 4.2) BA adsorption is favoured by the strong electrostatic interaction between the benzoate anion and the $–OH_2^+$ groups on the TiO_2 surface, which is positively charged at pH below the point of zero charge of TiO_2, i.e. pH_{zpc} 6.25 [25]. Therefore, the mononuclear bidentate chelate complex between the deprotonated carboxylic group of BA and a Ti(IV) surface atom can easily form [26]. At lower pH the extent of BA adsorption decreases because BA is prevalently undissociated and thus unable of electrostatic interaction with the protonated surface. Finally, in basic media strong repulsion is expected between the negatively charged titanium dioxide surface and the almost completely dissociated BA.

BA adsorption on ZnO at pH 9 was also negligible, though no repulsive interactions are expected in this case, the point of zero charge of this oxide being pH_{zpc}(ZnO) 9.3 [27]. Besides the lower surface area of ZnO (5 m^2 g^{-1}), also the fact that the complex between deprotonated BA and Zn(II) might be much weaker than that between BA and Ti(IV) may contribute to the lower adsorption of BA on ZnO.

3.2. FA and BA photocatalytic degradation on TiO_2

No detectable FA and BA photodegradation was evidenced in aqueous solutions in the absence of photocatalyst; thus, both acids are stable under UV irradiation in the emission range of the lamp. A significant decrease of the concentration of both substrates was observed instead under irradiation in the presence of 0.1 g L^{-1} of titanium dioxide: after 30 min irradiation at natural pH the residual amounts of FA and BA were 44 and 41%, respectively, of their initial concentration. BA photomineralisation of course proceeded at a lower rate, the residual TOC content being around 50% after 1 h.

During the runs, FA concentration always exhibited a constant rate decrease as a function of time, according to a zero-order rate law, in agreement with previous reports [24,28–30], while BA concentration decreased according to a pseudo first-order rate law. Tables 2 and 3 report the rate constants of the photocatalytic degradation of FA and BA, respectively, under different experimental conditions. These results are in agreement with a rate form of the Langmuir–Hinshelwood (L–H) type. As very recently demonstrated by Ollis in its illuminating approach to the problem [31], kinetic data fitting the L–H rate equation do not imply reactant adsorption on the photocatalyst to be equilibrated under irradiation. Indeed, the substantial reactivity of adsorbed

Table 2
Zero-order rate constants for the photocatalytic degradation of formic acid under different experimental conditions

Photocatalyst	pH	C^0_{FA} (M)	k (M s^{-1})
TiO_2	Natural[a]	5.0×10^{-4}	$(1.83 \pm 0.05) \times 10^{-7}$
TiO_2	Natural[a]	1.0×10^{-3}	$(1.87 \pm 0.03) \times 10^{-7}$
TiO_2	Natural[a]	2.0×10^{-3}	$(1.84 \pm 0.02) \times 10^{-7}$
TiO_2	2.6	5.0×10^{-4}	$(5.71 \pm 0.03) \times 10^{-8}$
TiO_2	9.0	5.0×10^{-4}	$(1.08 \pm 0.02) \times 10^{-7}$
TiO_2	10.0	5.0×10^{-4}	$(8.90 \pm 0.17) \times 10^{-8}$
ZnO	9.0	5.0×10^{-4}	$(6.1 \pm 0.2) \times 10^{-8}$
$TiO_2 + H_2O_2$[b]	Natural[a]	5.0×10^{-4}	$(4.6 \pm 0.2) \times 10^{-7}$

[a] Initial pH 3.5, final pH 5.8.
[b] H_2O_2 initial concentration: 2.5×10^{-4} M.

active species is expected to cause a continued displacement from equilibrium of the reactant concentration at the photocatalyst surface under illumination. According to this approach, the overall reaction rate can be expressed as:

$$r = k_2[\mathrm{OH}]\vartheta = k_2[\mathrm{OH}]\frac{K_a^{app}C}{1 + K_a^{app}C} \quad (1)$$

where k_2 is the rate constant for the adsorbed substrate reaction with surface active species (trapped holes or $^\bullet$OH radicals, formed by oxidation of water or OH^- anions by photoproduced valence band holes, assumed in steady state under irradiation), ϑ the surface coverage of reactant under irradiation, also assumed to be in pseudo-steady state, C the substrate concentration and K_a^{app} is the apparent binding constant on the illuminated photocatalyst:

$$K_a^{app} = \frac{k_1}{k_{-1} + k_2[\mathrm{OH}]} \quad (2)$$

k_1 and k_{-1} in Eq. (2) are the adsorption and desorption rate constants of the substrate on the illuminated catalyst surface. This novel approach [31] is consistent with the reported dependence of K_a^{app} values on radiation intensity, determining the concentration of photogenerated active sites on the semiconductor surface. It is worth underlining that such active sites exist only under illumination and that K_a^{app} may be markedly different [24,31] from the adsorption equilibrium constant of the substrate in the dark, K_a^d. By taking into account Eqs. (1) and (2), the L–H rate expression under steady state illumination conditions becomes:

$$r = \frac{k_1 k_2[\mathrm{OH}]C}{k_{-1} + k_2[\mathrm{OH}] + k_1 C} \quad (3)$$

Table 3
Pseudo first-order rate constants for the photocatalytic degradation of benzoic acid under different experimental conditions. $C^0_{BA} = 1.0 \times 10^{-4}$ M

Photocatalyst	pH	k (s^{-1})
TiO_2	2.6	$(4.3 \pm 0.2) \times 10^{-4}$
TiO_2	Natural[a]	$(4.97 \pm 0.08) \times 10^{-4}$
TiO_2	9.0	$(3.38 \pm 0.15) \times 10^{-4}$
ZnO	9.0	$(1.07 \pm 0.09) \times 10^{-3}$

[a] Initial pH 4.2, final pH 6.0.

The observed zero-order reaction for FA evidences that under irradiation the rate of FA adsorption on the photoactive sites is much higher than the sum of the two parallel paths concurring to decrease the amount of substrate at the photocatalyst surface, i.e. simple desorption and reaction with surface active species. This means that $k_1 C \gg k_{-1} + k_2[\mathrm{OH}]$ in Eq. (3). Indeed, almost identical zero-order rate constants of FA photocatalytic degradation were obtained starting from different initial FA concentrations (Table 2), in agreement with the absence of any mass transfer limitation. This indicates that the formic acid concentration ($C^0_{\mathrm{FA}} \geq 5 \times 10^{-4}$ M) employed in the present work in the presence of $0.1\,\mathrm{g\,L^{-1}}$ of photocatalyst is high enough to guarantee $K_a^{\mathrm{app}} C \gg 1$ in Eq. (1). Of course, this would not apply for the $K_a^{\mathrm{d}} C$ product under our experimental conditions. Indeed, the adsorption equilibrium constant of FA in the presence of $2\,\mathrm{g\,L^{-1}}$ of TiO_2 P25 has been recently found to be $3.16 \times 10^3\,\mathrm{M^{-1}}$ under dark condition [24]. Moreover, a L–H type saturating behaviour of the rate of FA photodegradation on TiO_2 was observed in an annular flow recirculating photocatalytic reactor [23] with increasing FA initial concentration, in the 1×10^{-4} to 2×10^{-3} M range. Thus, saturation conditions may well have been attained under irradiation in our experimental set-up.

We found that a not negligible amount of BA adsorbed on titanium dioxide in the absence of irradiation (Table 1). However, the binding constant of BA in the dark, measured in a water/methanol (90/10, v/v) mixture containing $0.5\,\mathrm{g\,L^{-1}}$ of colloidal TiO_2 at pH 3.6, has been reported to be $2 \times 10^3\,\mathrm{M^{-1}}$ [32], i.e. of the same order of that of FA.

When discussing the rate expression for the BA concentration decrease under photocatalysis, one should take into account that BA does not undergo direct mineralisation in one step, as is the case of FA. In fact, the photocatalytic degradation of BA proceeds through •OH radical attack preferentially on the *ortho* and *para* positions respect to the carboxylic group, producing hydroxy- and dihydroxy-benzoic acids, according to HPLC analysis. All such species may also interact with the irradiated photocatalyst, some of them (e.g. salicylic acid) also more strongly than BA [32], and undergo further photocatalytic degradation, in competition with BA, and final mineralisation through the aromatic ring opening upon further hydroxyl radical attacks [33]. Eq. (1) thus represents an approximation of the rate expression for the photocatalytically induced decrease of BA concentration, which is valid only for low concentration of intermediate species, i.e. at the beginning of the runs. Later on, the presence of such species causes a decrease of the ϑ value (several $K_{a,I}^{\mathrm{app}} C_I$ terms add to $1 + K_a^{\mathrm{app}} C_{\mathrm{BA}}$ in Eq. (1), C_I and $K_{a,I}^{\mathrm{app}}$ indicating in general the concentration of such intermediates and their apparent binding constant on the illuminated photocatalyst) and thus the slowing down of BA hydroxylation under irradiation. This contributes in yielding apparent pseudo first-order rate constants, whose values decrease with increasing the initial substrate concentration [34].

Indeed, progressively lower pseudo first-order rate constants k of BA photocatalytic degradation were measured, starting from progressively higher initial BA concentrations C^0_{BA}, in the 1.9×10^{-5} to 1.27×10^{-4} M range. However, by plotting the initial photocatalytic degradation rate, evaluated as $r_0 = kC^0_{\mathrm{BA}}$, as a function of C^0_{BA}, we find the typical saturating behaviour depicted in Fig. 1, in the frame of a L–H rate form. Thus, in the case of BA, an initial concentration $C^0_{\mathrm{BA}} \geq 1.5 \times 10^{-4}$ M is required to attain photocatalytic rate saturation under the irradiation conditions of the present work. These results are fully compatible with those very recently reported with a different TiO_2 sample [35], showing a broad rate maximum for an initial BA concentration around 4×10^{-4} M.

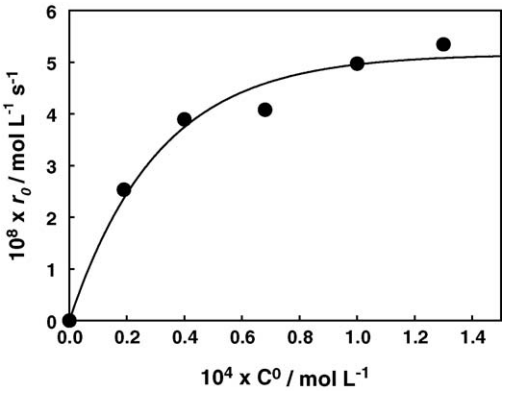

Fig. 1. Effect of the initial BA concentration on the initial rate of BA photocatalytic degradation on TiO_2, evaluated as $r_0 = kC^0_{\mathrm{BA}}$.

3.3. pH effects on FA and BA photodegradation on TiO_2

FA and BA photocatalytic degradation runs were performed on TiO_2 at different pH, ranging between 2.6 and 10.0; the rate constants obtained at different pH are reported in Tables 2 and 3 and plotted versus pH in Figs. 2 and 3.

The degradation rate of both substrates was maximum at natural pH and decreased at both lower and higher pH. The observed trends are clearly correlated to the electrostatic interactions between the substrate and the photocatalyst surface, depending on the pH of the suspension [36], as already pointed out in Section 3.1. In the range between the zero point charge of TiO_2 ($\mathrm{pH_{zpc}}$ 6.25 [25]) and the $\mathrm{p}K_a$ values of the two acids (3.75 for FA and 4.19 for BA), the substrate–surface electrostatic attraction is maximum. At pH below their $\mathrm{p}K_a$ val-

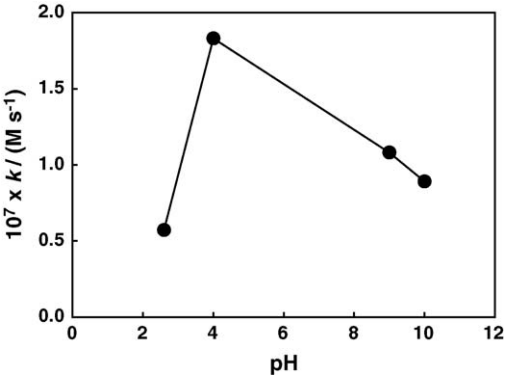

Fig. 2. Effect of pH on the zero-order rate constants of FA photocatalytic degradation on TiO_2; $C^0_{\mathrm{FA}} = 5.0 \times 10^{-4}$ M.

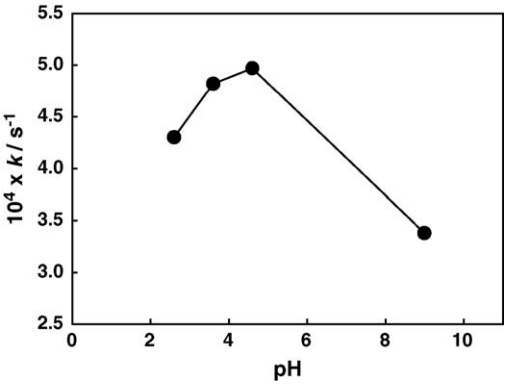

Fig. 3. Effect of pH on the pseudo first-order rate constants of BA photocatalytic degradation on TiO_2; $C^0_{BA} = 1.0 \times 10^{-4}$ M.

ues the substrates experience neither attraction nor repulsion from the oxide surface, while formate and benzoate anions are repelled from the negatively charged photocatalyst surface at pH above the pH_{zpc} of TiO_2, according to a simple surface charge model.

These electrostatic interactions have a significant influence on the photocatalytic degradation rate of the two substrates, as they determine their space distribution close to the semiconductor surface, where the photogenerated active species are mainly confined. The main photodegradative paths for both FA and BA in the present conditions should be the reaction with the surface-bound •OH radicals photogenerated through water (or hydroxyl anions) oxidation by valence band holes or the direct electron transfer to the semiconductor valence band holes. Both processes are expected to be inhibited by a longer distance between substrate and oxide surface. Oxidation via homogeneous hydroxyl radicals should be excluded, as it is expected to eventually become more favourable at a higher pH [37].

Based on the above discussion, we should expect a higher degradation rate under acidic conditions (no electrostatic interactions) than under basic (repulsive) conditions, but this is true only for BA and not for FA. This effect should be ascribed to the different reactivity of surface-bound hydroxyl radicals for the dissociated and undissociated form of the two acids, leading to hydrogen abstraction in the case of FA and to OH addition to the aromatic ring in the case of BA. In fact, the rate constant of the aqueous phase •OH radical attack on undissociated FA is $1.3 \times 10^8\ M^{-1}\ s^{-1}$, which is more than one order of magnitude lower compared to the rate constant of •OH radical attack on the formate anion ($3.2 \times 10^9\ M^{-1}\ s^{-1}$) [38]. On the contrary, the rate constants of hydroxyl radical attack on benzoic acid and on the benzoate anion have higher and much closer values (4.3×10^9 and $5.9 \times 10^9\ M^{-1}\ s^{-1}$, respectively) [38].

The band shift to more reducing potentials, occurring as the pH increases, in principle may also affect the rate of substrate degradation. In fact, the valence band potential, ca. 2.9 V versus NHE at pH 3, decreases 0.059 V for each unit increase in pH. However, it always remains positive enough to oxidise FA and BA (for instance, $E_{CO_2/HCOOH} = -0.40$ V versus NHE at pH 3 [12]).

3.4. Hydrogen peroxide evolution during FA and BA photodegradation on TiO_2

The evolution of hydrogen peroxide during the photocatalytic degradation runs was also followed under different pH conditions, to ascertain the existence of a correlation between the rates of FA and BA oxidative degradation and that of the main parallel reductive path occurring under irradiation. Of course, hydrogen peroxide could be detected in the photocatalytic reaction system only if its formation rate was greater than its consumption rate under irradiation [39]. H_2O_2 has been shown to form in irradiated suspensions via reduction of molecular oxygen by conduction band electrons [40] and it can be photocatalytically degraded mainly on the photocatalyst surface by photogenerated charged species, i.e. holes and electrons, by hydroxyl radicals and by the superoxide radical anion [41–43]. In particular, the photocatalytic reduction of H_2O_2 by conduction band electrons has been recently demonstrated to lead to the formation of extra •OH radicals [43]. Hydrogen peroxide may also undergo the photoinduced scission of the O–O bond in the aqueous phase, also producing hydroxyl radicals; such reaction, however, was found to be negligible under our irradiation conditions.

During FA photodegradation, no H_2O_2 was detected in the aqueous phase regardless of pH, i.e. its concentration was lower than the detection limit of the analytical method employed in the present work (0.16 μM). On the contrary, relatively high H_2O_2 concentrations could be detected during BA photocatalytic degradation especially under acidic conditions, as shown in Fig. 4.

No evidence of H_2O_2 formation was reported in earlier studies on the photocatalytic decomposition of FA [5,33]. Only a ppm level of such species has very recently been detected by Shiraishi et al. [44] during the photocatalytic degradation of FA on TiO_2 thin films in an annular flow photocatalytic reactor. The same authors have also evidenced that photoproduced H_2O_2 is quickly decomposed within the thin film surrounding the photocatalyst, so that its concentration in the bulk liquid could hardly become high enough to be detected under batch reaction conditions [45].

Thus, hydrogen peroxide could not be detected by us during FA photocatalytic degradation because of its fast decomposition

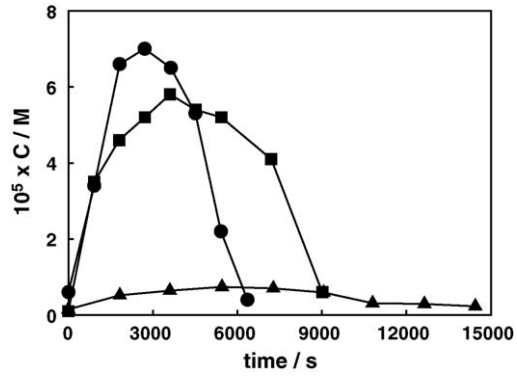

Fig. 4. Hydrogen peroxide evolution during BA photodegradation on TiO_2 at natural pH (●), at pH 2.6 (■) and at pH 9 (▲); $C^0_{BA} = 1.0 \times 10^{-4}$ M.

on the oxide surface, yielding no stable intermediate species. When the photocatalyst surface is not significantly protected by adsorbed molecules, titanium–peroxo complexes ($\equiv Ti^{IV}-OOH$) [46] can form and the electron transfer of photogenerated species, able to reduce or oxidise the peroxo group, is favoured. Adsorption tests evidenced that in an aqueous suspension containing 0.1 g L^{-1} of TiO_2 and 1.4×10^{-4} M hydrogen peroxide ca. 30% of this latter is adsorbed on the oxide at equilibrium in the dark. This result is fully compatible with the very recently reported adsorption isotherm of H_2O_2 at pH 4 in the presence of 5 g L^{-1} of TiO_2 [47]. Of course, hydrogen peroxide adsorption on the photocatalyst contributes in increasing its detection limit in the system, our fluorimetric analysis determining only the free, unadsorbed H_2O_2 in the aqueous phase.

On the other hand, BA and its photooxidation intermediates compete with H_2O_2 for adsorption on the semiconductor, thus contributing to slow down its photocatalytic degradation. In fact, as shown in Fig. 4, a relatively high amount of peroxide was detected during BA photodegradation at natural pH, i.e. under conditions of maximum BA degradation rate (Table 3) and rather low H_2O_2 decomposition rate [42]. The initial rate of H_2O_2 formation was almost identical at pH 2.6, but the hydrogen peroxide concentration profile started to decline at longer irradiation time. Both the lower rate of H_2O_2 photodecomposition on TiO_2, which has been reported to decrease with decreasing pH, at least under visible irradiation [42], and the lower rate of BA oxidative degradation (Table 3) contribute to this effect. Indeed, the longer persistence of organic species, able to capture photoproduced valence band holes, guarantees a prolonged availability of conduction band electrons for O_2 reduction and consequent H_2O_2 production, and also hinders H_2O_2 photodecomposition on TiO_2. A comparison between the H_2O_2 concentration profiles (Fig. 4) and the residual TOC content in BA irradiated suspensions (Fig. 5) clearly points to this conclusion. Finally, very low amounts of H_2O_2 were detected for a relatively long lapse of time at basic pH: under these conditions not only BA adsorption was extremely low and its degradation slow, but H_2O_2 adsorption and photodecomposition were greatly favoured [42].

Thus, the adsorption of substrates and intermediates on the photocatalyst surface directly affects the interaction of H_2O_2 with the TiO_2 particles and consequently its decomposition rate. Relatively good adsorption and high photocatalytic degradation rate of the substrate are prerequisites for H_2O_2 accumulation under photocatalytic conditions. Indeed, the higher was the rate of BA decomposition, the higher was the H_2O_2 amount, confirming that it forms through a reductive route, parallel to the oxidative degradation of BA.

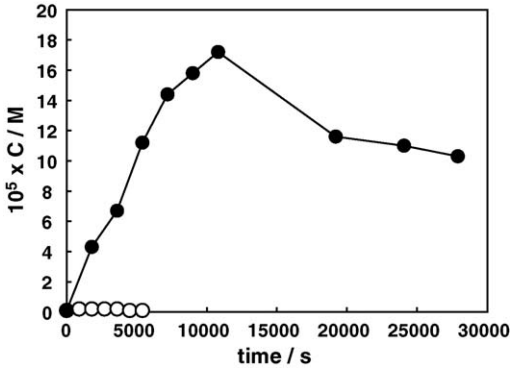

Fig. 6. Hydrogen peroxide evolution during FA photodegradation at pH 9 on TiO_2 (◯) and on ZnO (●); $C^0_{FA} = 5.0 \times 10^{-4}$ M.

3.5. FA and BA photodegradation on ZnO

The rate constants of FA and BA photocatalytic degradation in the presence of zinc oxide at pH 9 are also collected in Tables 2 and 3, while hydrogen peroxide concentration profiles on the two oxides are compared in Figs. 6 and 7. FA photocatalytic degradation on ZnO was slower than on TiO_2 at similar pH; on the contrary, for BA a much higher degradation rate was observed on ZnO, leading to a greater accumulation of hydroxylated intermediate species and to a higher mineralisation rate. For both substrates the amount of hydrogen peroxide generated on zinc oxide was much higher than on titanium dioxide.

To have a deeper insight into the origin of such effects, hydrogen peroxide formation in irradiated TiO_2 and ZnO suspensions was investigated also in the absence of any organic substrate. As shown in Fig. 8, the removal of organic molecules undergoing photocatalytic oxidation completely suppressed H_2O_2 evolution on TiO_2 under our experimental conditions. By contrast, H_2O_2 could easily be detected in irradiated ZnO suspensions and its concentration increased with irradiation time, up to a

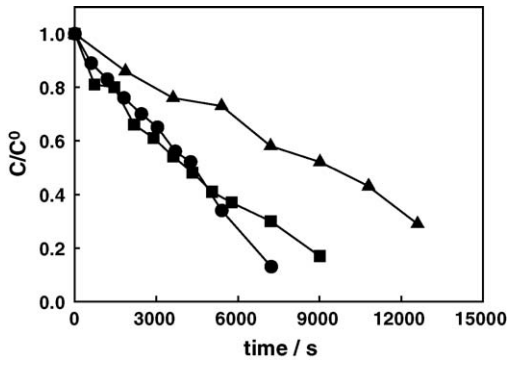

Fig. 5. Residual total organic carbon content during BA photodegradation on TiO_2 at natural pH (●), at pH 2.6 (■) and at pH 9 (▲); $C^0_{BA} = 1.0 \times 10^{-4}$ M.

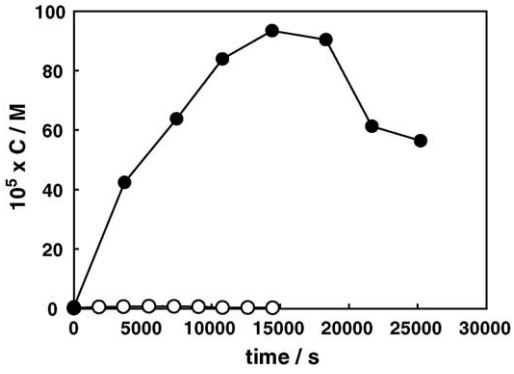

Fig. 7. Hydrogen peroxide evolution during BA photodegradation at pH 9 on TiO_2 (◯) and on ZnO (●); $C^0_{BA} = 1.0 \times 10^{-4}$ M.

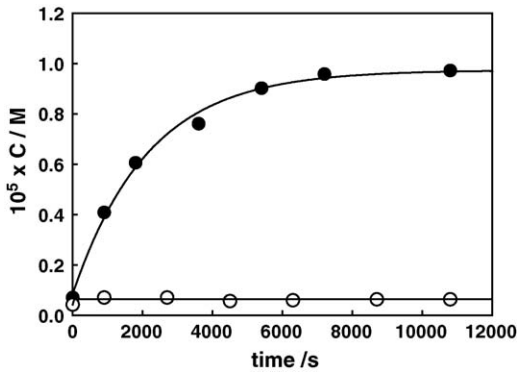

Fig. 8. Hydrogen peroxide evolution under irradiation of aqueous suspensions containing 0.1 g L^{-1} of TiO_2 (◯) and of ZnO (●) at pH 9.

steady value around 1×10^{-5} M, which is much lower than those attained on this oxide in the presence of the two substrates. The higher concentrations of H_2O_2 in irradiated ZnO suspensions are a consequence not only of the relatively high quantum yield of H_2O_2 formation, but also of the relative inefficiency of H_2O_2 photocatalytic degradation on this oxide, in comparison with TiO_2 [22]. In the absence of species able to combine with photogenerated valence band holes, thus increasing the availability of conduction band electrons for adsorbed dioxygen reduction, the rate of H_2O_2 formation is expected to be reduced on both photocatalysts. At the same time, the rate of its photoinduced degradation on the photocatalyst bare surface is expected to increase, because of the lack of adsorbed molecules competing with hydrogen peroxide for adsorption. H_2O_2 accumulation on TiO_2 is mainly compromised by this second effect.

Moreover, during FA photocatalytic degradation on TiO_2 the fast and complete degradation of H_2O_2 generates reactive species on the surface of the semiconductor particles, contributing to the effectiveness of the photocatalytic process. Indeed, the so generated surface-bound $^{\bullet}$OH radicals [43] may contribute to the enhancement of the FA degradation rate. On the contrary, hydrogen peroxide does not appreciably decompose on ZnO and consequently it does not generate extra hydroxyl radicals; this may explain the lower photodegradation rate of FA on zinc oxide, compared to titanium dioxide [48]. Indeed, the addition to TiO_2 suspensions of 2.5×10^{-4} M H_2O_2, a concentration comparable to that formed in situ under photocatalytic conditions, produced a remarkable increase of the FA photocatalytic degradation rate (Table 2). On the contrary, the addition of H_2O_2 has been reported to have no effect on the rate of photocatalytic degradation of different substrates on ZnO [48,49].

Conversely, BA exhibited the highest photocatalytic reactivity on ZnO at pH 9. As shown in Table 3, the rate constant value obtained under such conditions was more than double respect to that measured in TiO_2 suspensions at natural pH. Of course, this excludes any relevant role of the photocatalytic decomposition of H_2O_2 at the interface, as it would lead to just the opposite effect. The above discussed net charge on the oxide surfaces, regulating BA affinity for them, may explain the higher photocatalytic reactivity of BA on ZnO respect to TiO_2 at pH 9. In fact, because of the higher value of the zero point charge of ZnO (pH_{zpc} 9.3), at pH 9 the benzoate anion experiences electrostatic attraction for the photocatalyst surface, of the same type occurring at the TiO_2–water interface for $pK_a < pH < pH_{zpc}$. It can thus reside in the interface zone close to the particles surface and readily interact with the photogenerated active species.

However, also taking into account such favourable electrostatic effects, ZnO appears to be an intrinsically more effective photocatalyst than TiO_2 for BA degradation; a similar effect has already been noticed in the photocatalytic degradation of azo dyes and other aromatic compounds [6,20,50]. A possible explanation of this finding is that the lower adsorption of BA on ZnO, respect to TiO_2, retards the recombination reaction between conduction band electrons and the $BA^{+\bullet}$ species, formed at the photocatalyst surface by monoelectronic oxidation of BA [51], thus increasing the rate of its further oxidation.

4. Conclusions

By monitoring the photocatalytic oxidative degradation of FA and BA on TiO_2 and ZnO and the simultaneous H_2O_2 evolution, proceeding through a reductive path started by conduction band electrons, we ascertained that for BA on TiO_2 a correlation exists between the two processes, and that the adsorption of BA and of its degradation intermediates plays a key role in the photocatalytic evolution of hydrogen peroxide. FA, giving no stable photocatalytic degradation intermediates, does not guarantee a sufficient shielding of the TiO_2 surface, where H_2O_2 undergoes quite fast photoinduced decomposition through ≡Ti–OOH complexes. ZnO is more effective than TiO_2 for BA, but not for FA photocatalytic degradation. Much higher amounts of hydrogen peroxide accumulate in ZnO irradiated suspensions, both in the presence and in the absence of the two substrates, mainly because of its lower photoreactivity on such oxide.

References

[1] M.A. Fox, M.T. Dulay, Chem. Rev. 93 (1993) 341.
[2] M.R. Hoffmann, S.T. Martin, W.Y. Choi, D.W. Bahnemann, Chem. Rev. 95 (1995) 69.
[3] A. Fujishima, T.N. Rao, D.A. Tryk, J. Photochem. Photobiol. C: Photochem. Rev. 1 (2000) 1.
[4] S.R. Morrison, T. Freund, J. Phys. Chem. 47 (1967) 1543.
[5] C. Richard, P. Boule, J.M. Aubry, J. Photochem. Photobiol. A: Chem. 60 (1991) 235.
[6] E. Selli, Phys. Chem. Chem. Phys. 4 (2002) 6123.
[7] M. Mrowetz, C. Pirola, E. Selli, Ultrason. Sonochem. 10 (2003) 247.
[8] M. Mrowetz, E. Selli, J. Photochem. Photobiol. A: Chem. 162 (2004) 89.
[9] M. Bertelli, E. Selli, Appl. Catal. B: Environ. 52 (2004) 205.
[10] R.W. Matthews, Water Res. 24 (1990) 653.
[11] L. Davydov, P.G. Smirniotis, J. Catal. 191 (2000) 105.
[12] R.J. Candal, W.A. Zeltner, M.A. Anderson, Environ. Sci. Technol. 34 (2000) 3443.
[13] D.S. Muggli, M.J. Backes, J. Catal. 209 (2002) 105.
[14] I. Izumi, F.-R. Fan, A.J. Bard, J. Phys. Chem. 85 (1981) 218.
[15] R.W. Matthews, J. Chem. Soc., Faraday Trans. 1 80 (1984) 457.
[16] V. Brezová, M. Čeppan, E. Brandšteterová, M. Breza, L. Lapčik, J. Photochem. Photobiol. A: Chem. 59 (1991) 385.
[17] V. Ragaini, E. Selli, C.L. Bianchi, C. Pirola, Ultrason. Sonochem. 8 (2001) 251.

[18] C.G. Hatchard, C.A. Parker, Proc. R. Soc. (Lond.) A235 (1956) 518.
[19] M. Abdullah, J.K.C. Low, R.W. Matthews, J. Phys. Chem. 94 (1990) 6820.
[20] A.A. Khodja, T. Sehili, J.F. Pilichowski, P. Boule, J. Photochem. Photobiol. A: Chem. 141 (2001) 231.
[21] G.G. Guilbault, P.J. Brignac Jr., M. Juneau, Anal. Chem. 40 (1968) 1256.
[22] C. Kormann, D.W. Bahnemann, M.R. Hoffmann, Environ. Sci. Technol. 22 (1988) 798.
[23] S. Wang, F. Shiraishi, K. Nakano, J. Chem. Technol. Biotechnol. 77 (2002) 805.
[24] N. Serpone, J. Martin, S. Horikoshi, H. Hidaka, J. Photochem. Photobiol. A: Chem. 169 (2005) 235.
[25] C. Kormann, D.W. Bahnemann, M.R. Hoffmann, Environ. Sci. Technol. 25 (1991) 494.
[26] S. Tunesi, M.A. Anderson, Langmuir 8 (1992) 487.
[27] D.W. Bahnemann, C. Kormann, M.R. Hoffmann, J. Phys. Chem. 91 (1987) 3789.
[28] M. Bideau, B. Claudel, M. Otterbein, J. Photochem. 14 (1980) 291.
[29] G. Chester, M. Anderson, H. Read, S. Esplugas, J. Photochem. Photobiol. A: Chem. 71 (1993) 291.
[30] M.F.J. Dijkstra, A. Michorius, H. Buwalda, H.J. Panneman, J.G.M. Winkelman, A.A.C.M. Beenackers, Catal. Today 66 (2001) 487.
[31] D.F. Ollis, J. Phys. Chem. B 109 (2005) 2439, and references therein.
[32] J. Moser, S. Punchilewa, P.P. Infelta, M. Grätzel, Langmuir 7 (1991) 3012.
[33] A.A. Ajmera, S.B. Sawant, V.G. Pangarkar, A.A.C.M. Beenackers, Chem. Eng. Technol. 25 (2002) 173.
[34] D.F. Ollis, E. Pelizzetti, N. Serpone, in: N. Serpone, E. Pelizzetti (Eds.), Photocatalysis. Fundamentals and Applications, Wiley, New York, 1989, p. 603.
[35] D. Vione, C. Minero, V. Maurino, M.E. Carlotti, T. Picanotto, E. Pelizzetti, Appl. Catal. B: Environ. 58 (2005) 79.
[36] D.H. Kim, M.A. Anderson, J. Photochem. Photobiol. A: Chem. 94 (1996) 221.
[37] S. Kim, W.Y. Choi, Environ. Sci. Technol. 36 (2002) 2019.
[38] G.V. Buxton, C.L. Greenstock, W.P. Helman, A.B. Ross, J. Phys. Chem. Ref. Data 17 (1988) 513.
[39] I. Ilisz, K. Föglein, A. Dombi, J. Mol. Catal. A: Chem. 135 (1998) 55.
[40] A.J. Hoffmann, E.R. Carraway, M.R. Hoffmann, Environ. Sci. Technol. 28 (1994) 776.
[41] B. Jenny, P. Pichat, Langmuir 7 (1991) 947.
[42] X. Li, C. Chen, J. Zhao, Langmuir 17 (2001) 4118.
[43] T. Hirakawa, Y. Nosaka, Langmuir 18 (2002) 3247.
[44] F. Shiraishi, T. Nakasako, Z. Hua, J. Phys. Chem. B 107 (2003) 11072.
[45] F. Shiraishi, C. Kawanishi, J. Phys. Chem. B 108 (2004) 10491.
[46] G. Munuera, A.R. Gonzalez-Elipe, J. Soria, J. Sanz, J. Chem. Soc., Faraday Trans. 76 (1980) 1535.
[47] V. Maurino, C. Minero, G. Mariella, E. Pelizzetti, Chem. Commun. (2005) 2627.
[48] L. Amalric, C. Guillard, P. Pichat, Res. Chem. Intermed. 20 (1994) 579.
[49] S. Rabindranathan, S. Devipriya, S. Yesodharan, J. Hazard. Mater. 102 (2003) 217.
[50] C. Lizama, J. Freer, J. Baeza, H.D. Mansilla, Catal. Today 76 (2002) 235.
[51] C. Minero, Catal. Today 54 (1999) 205.